



Chapter 4

X-RAY RADIATION PHENOMENA

INTRODUCTION

4-1 Production of X-Rays

X-rays are electromagnetic radiations of frequencies from about 10^{16} Hz* to about 10^{20} Hz, overlapping ultraviolet radiation at the low frequency end of the spectrum and gamma rays at the high end (see Figure 4-1). The wavelengths of the radiations are given by

$$\lambda = c/\nu \text{ cm.}$$

where ν is the frequency in Hz, and c is the velocity of light (3×10^{10} cm per sec). X-rays exhibit particle-like properties as well as wave-like properties, and are absorbed or emitted in quanta, or photons, of energy

$$E = h\nu \text{ ergs.}$$

where h is Planck's constant (6.625×10^{-27} erg-sec). This energy is ordinarily expressed in kiloelectron-volts (keV).† Figure 4-2 shows X-ray wavelength and frequency as a function of photon energy. The more energetic X-rays of higher frequency are commonly known as "hard" X-rays, and the less energetic ones are correspondingly "soft."

The distinction between X-rays and other electromagnetic radiations is not made in terms of their respective frequencies but in terms of their method of production. Gamma rays, for instance, are those photons produced as a result of nuclear forces, whereas production of X-rays is associated with electromagnetic forces acting on electrons. Two basic physical mech-

anisms are principally responsible for X-ray production; the corresponding emissions are bremsstrahlung (braking radiation) and the characteristic radiation.

Bremsstrahlung is a result principally of inelastic (or radiative) scattering of fast electrons by atoms. If a beam of monoenergetic electrons impinges on a thick target, a spectrum of X-rays is produced with maximum energy equal to that of the electrons and a spectral distribution that depends on the atomic number, Z , of the target.

The spectrum of X-rays from such an experiment will contain (in addition to the bremsstrahlung spectrum) a number of intense, fairly sharp spectral lines. These lines are characteristic of the material being bombarded and result from X-rays that are emitted when the atomic electrons rearrange themselves into states of lower energy after one or more electrons have been knocked out of the atom by the bombarding electrons. Since the atomic electrons must be in one of a number of discrete energy stages, transitions between the states are accomplished by emissions of photons of discrete energies. If the initial beam has sufficient energy to remove the most tightly bound (K-shell) electrons from the atom, all possible transitions between states will result in X-rays and all of the characteristic spectral lines will be seen. At slightly lower incident beam energies, the K X-ray lines will disappear but the other lines will still be observed, and so on. The frequencies of the characteristic radiation depend on the atomic numbers of the

*1 Hz (Hertz) = 1 cycle per second.

†1 keV = 10^3 ev; 1 ev = 1.6×10^{-12} erg.

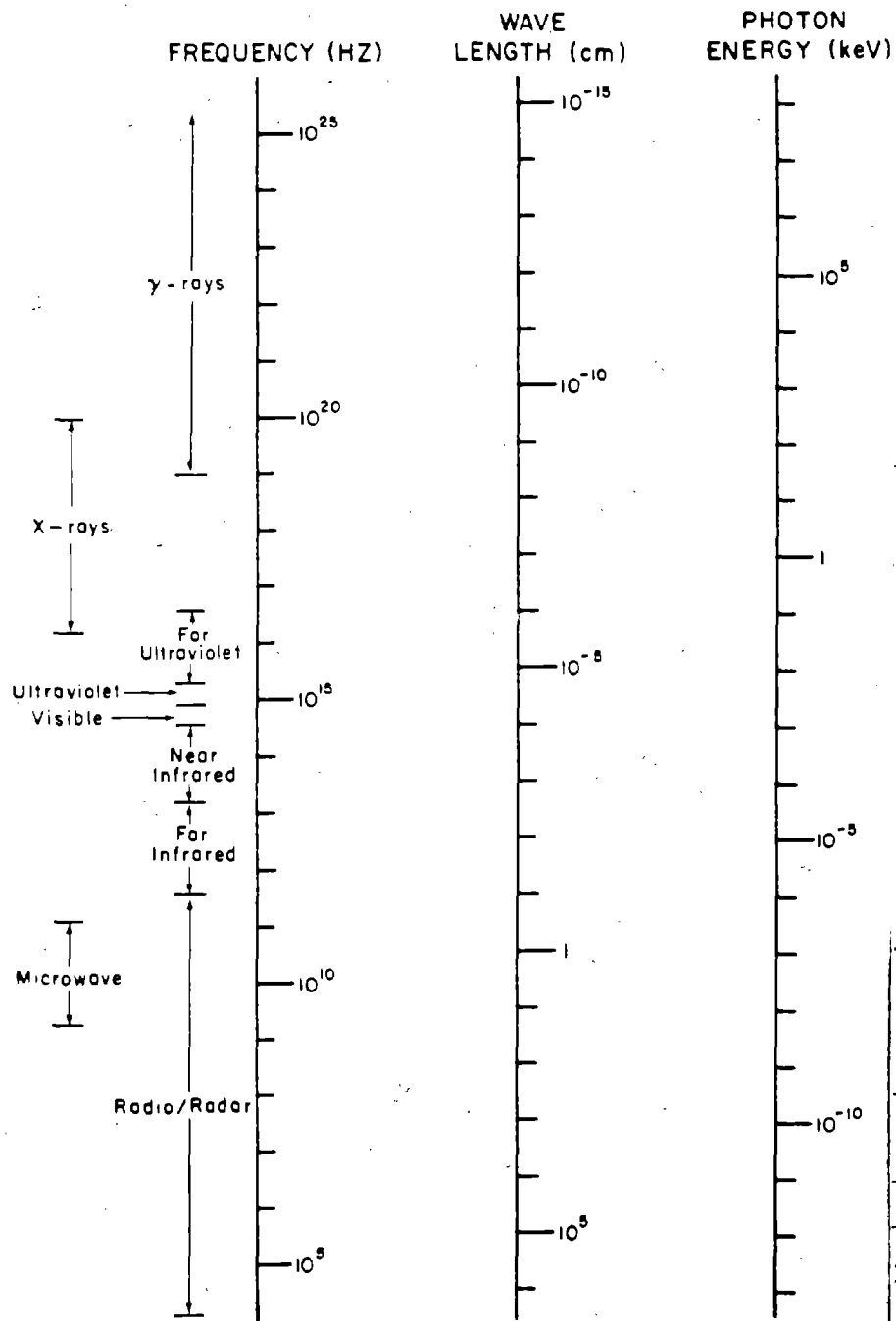


Figure 4-1. Properties of Electromagnetic Radiation

| | |
|--------------------|-------------------------------------|
| Accession For | |
| NTIS GRA&I | <input checked="" type="checkbox"/> |
| DTIC TAB | <input type="checkbox"/> |
| Unannounced | <input type="checkbox"/> |
| Justification | <i>Basic Doc</i> |
| By _____ | |
| Distribution/ | |
| Availability Codes | |
| Dist | Avail and/or Special |
| | |

A-1

UNANNOUNCED



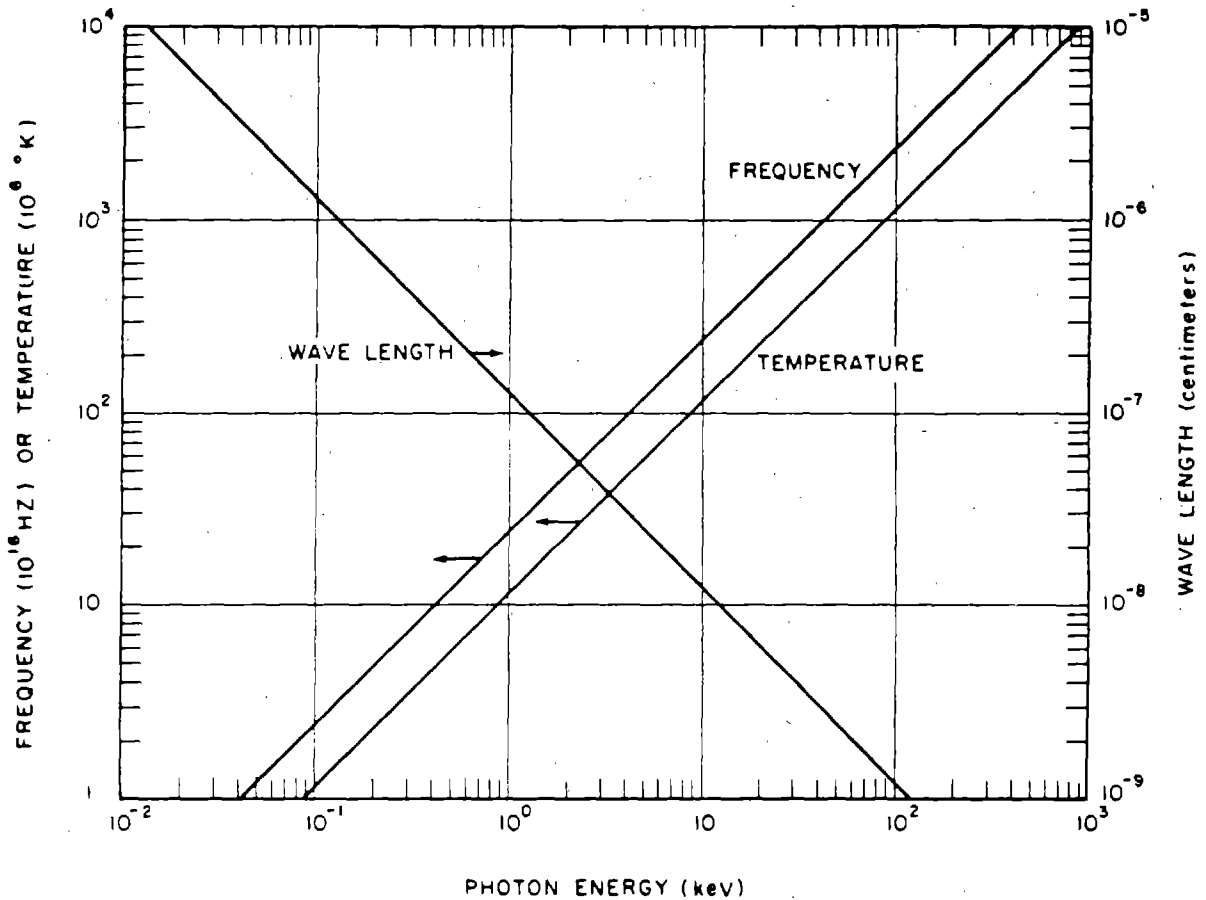


Figure 4-2. Wavelength, Frequency, and Temperature as a Function of Electromagnetic Photon Energy

target materials: the higher the atomic number, the higher is the frequency and energy of the hardest characteristic X-ray.

4-2 Black Body Radiation

The mechanism whereby an atom is ionized (loses one or several electrons) does not alter the characteristics of the X-rays emitted as the ionized atom deexcites (recaptures electrons). An X-ray can be produced no matter whether the ionization is produced by an inci-

dent fast electron or by any other process leaving an unfilled energy level. Similarly, any process whereby fast electrons are decelerated rapidly can produce X-ray bremsstrahlung. Both types of conditions are found in high temperature plasmas, which are composed of molecules, atoms, ions, electrons, and accompanying electromagnetic radiation, all in a state of thermal excitation corresponding to the temperature of the plasma. The hotter the plasma, the less likely it is that nonionized atoms and molecules will be

present, and the more likely will be the presence of multiply ionized atoms. At very high temperatures, the atoms can become completely ionized, leaving only bare nuclei and electrons in the plasma. Under such conditions, the possible frequencies of "characteristic" X-rays become essentially a continuum, both because so many energy states are unfilled and because the thermal motions of the nuclei cause Doppler shifts in the frequencies of the emitted lines. The resultant radiation is similar to that from any hot gas, except that the plasma can be enormously hotter and therefore can emit much higher frequencies, including X-rays, as well as ultraviolet, visible, and infrared radiations.

Plasmas are, in general, very complex, and the spectral distributions of the radiation emitted from them are correspondingly complex. However, much insight can be gained by studying a simpler, idealized thermal radiator, the black body. This does not mean that radiation from a plasma can be characterized by a black body, but in some cases a black body provides a rough approximation. Black body radiation is that seen emerging through a small hole in the wall of a hollow body at a constant temperature. It is also known as isothermal cavity radiation. Black body radiation has been studied extensively both experimentally and theoretically, and the following results are of interest.

(U) The total power emitted per unit area of a black body at absolute temperature T is

$$\Phi_s = \sigma T^4 \text{ erg-sec}^{-1}\text{-cm}^2$$

where the Stefan-Boltzmann constant σ is equal to $5.67 \times 10^{-5} \text{ erg sec}^{-1} \text{ cm}^{-2} \text{ }^\circ\text{K}^{-4}$.

The theoretical explanation of the observed distribution of the frequencies of the radiation depended on the quantum hypothesis advanced by Planck, and the energy spectrum is generally referred to as a Planck spectrum. The Planck spectrum, in terms of the energy density

radiated between wavelengths λ and $\lambda + d\lambda$, is

$$\Psi(\lambda)d\lambda = \frac{8\pi ch}{\lambda^5} \frac{d\lambda}{e^{(ch/\lambda kT)} - 1}$$

where all symbols are as previously defined, except that k is the Boltzmann constant and is equal to $1.38 \times 10^{-16} \text{ erg/}^\circ\text{K}$. The Planck spectrum can also be expressed in terms of the power emitted per unit area per unit frequency for photons with frequencies between ν and $\nu + d\nu$ as

$$\Phi_s(\nu)d\nu = \frac{2\pi\nu^2 d\nu}{c^2} \frac{h\nu}{e^{(h\nu/kT)} - 1}$$

Since both $h\nu$ and kT have the dimensions of energy (and can be expressed in keV), the spectral distribution can be expressed in terms of the normalized energy (a dimensionless parameter) $u = h\nu/kT$ as

$$\Phi_s(u)du = \sigma T^4 F(u)du$$

where use has been made of the Stefan-Boltzmann equation, and

$$F(u) = \frac{15\pi^4 u^3}{e^u - 1}$$

is called the density function of the normalized Planck distribution. The quantity $F(u)du$ is the fraction of the total radiation emitted by a black body at temperature T between the frequencies ν and $\nu + d\nu$, where $\nu = u(kT/h)$.

The fraction of photons with energies less than $h\nu$ is therefore

$$G(u) = \int_0^u F(u')du'$$

$G(u)$ is called the cumulative distribution func-

Table 4-1. Normalized Planck Distribution

| Normalized Energy, u | Density Function, $F(u)$ | Cumulative Distribution Function, $G(u)$ |
|------------------------|--------------------------|--|
| 0.5 | 2.9674×10^{-2} | 5.2932×10^{-3} |
| 1.0 | 8.9627×10^{-2} | 3.4618×10^{-2} |
| 1.5 | 1.4928×10^{-1} | 9.4780×10^{-2} |
| 2.0 | 1.9283×10^{-1} | 1.8114×10^{-1} |
| 2.5 | 2.1519×10^{-1} | 2.8402×10^{-1} |
| 2.82 (u_{\max}) | 2.1890×10^{-1} | 3.5368×10^{-1} |
| 3.0 | 2.1787×10^{-1} | 3.9301×10^{-1} |
| 4.0 | 1.8389×10^{-1} | 5.9702×10^{-1} |
| 5.0 | 1.3059×10^{-1} | 7.5453×10^{-1} |
| 6.0 | 8.2660×10^{-2} | 8.6016×10^{-1} |
| 7.0 | 4.8212×10^{-2} | 9.2442×10^{-1} |
| 8.0 | 2.6459×10^{-2} | 9.6084×10^{-1} |
| 9.0 | 1.3857×10^{-2} | 9.8038×10^{-1} |
| 10.0 | 6.9920×10^{-3} | 9.9045×10^{-1} |

tion (note that $G(\infty) = 1$ for all temperatures). The functions $F(u)$ and $G(u)$ are tabulated in Table 4-1 and plotted in Figure 4-3. The maximum of the density function occurs at $u_{\max} = 2.82144$. Other useful relationships are that only about three and a half percent of the radiation occurs at energies below kT ($u = 1$), and only about thirty-five percent below the peak of the spectrum ($u = 2.82$). Only one percent of the energy is radiated in photons with energies greater than ten times the black body temperature

(kT), i.e., for $u \geq 10$. The median energy is at about $u = 3.5$.

Ideal black bodies produce some radiation at all frequencies. In order for significant quantities of X-rays to be produced, however, the temperature of the black body must be great enough that u_{\max} occurs in the X-ray region, i.e., for the $h\nu \sim .3$ keV or greater. This implies that $kT > 0.1$ keV or that T must be greater than about a million degrees Kelvin.

[REDACTED]

Problem 4-1. Calculation of Spectral Distribution and Cumulative Emissions from Black Body Sources

Figure 4-3 and Table 4-1 show the normalized energy distribution and the normalized cumulative energy function for black body radiators. These normalized functions may be applied to black body radiators of various temperatures expressed in any unit of temperature measure. The common unit of temperature measure for high temperature plasmas is keV.

Scaling

a. To find the fraction of total energy emitted at a specified photon energy, $h\nu$, divide the specified photon energy by the black body source temperature, kT , to obtain the normalized energy, u ,

$$u = \frac{h\nu}{kT}$$

Enter Figure 4-3 with the normalized energy, and read the fraction of the total energy emitted at the specified energy from the density function curve.

b. To find the cumulative fraction of energy emitted at or below a specified photon energy, $h\nu$, divide the specified photon energy by the black body source temperature, kT , to obtain the normalized energy, u ,

$$u = \frac{h\nu}{kT}$$

Enter Figure 4-3 with the normalized energy, and read the cumulative fraction of energy emitted at or below the specified photon energy from the cumulative distribution function curve.

Example

Given:

a. A black body radiating at a temperature of 2 keV.

b. A black body radiating at a temperature of 3 keV.

Find:

a. The photon energy that is emitted with the greatest frequency from the 2 keV black body.

b. The photon energy at which 65 percent of the total energy emitted contains photons of that energy or lower from the 3 keV black body.

Solution:

a. From Figure 4-3 (or Table 4-1), the peak emission occurs at a normalized energy of

$$u = 2.82.$$

b. From Figure 4-3, 65 percent of the energy is emitted at normalized energies equal or less than

$$u = 4.3.$$

Answer:

a. The photon energy that is emitted with greatest frequency from a 2 keV black body radiator is

$$h\nu = 2.82 kT = (2.82)(2) = 5.64 \text{ keV.}$$

b. Sixty-five percent of the photons from a 3 keV black body radiator have energies equal to or less than

$$h\nu = 4.3 kT = (4.3)(3) = 12.9 \text{ keV}$$

(Thirty-five percent of the photons will have energies greater than 12.9 keV.)

Reliability: Figure 4-3 represents the density function and cumulative distribution function of theoretically ideal black body radiators. Actual radiators will deviate from the ideal.

Related Material: See paragraphs 4-1 and 4-2.

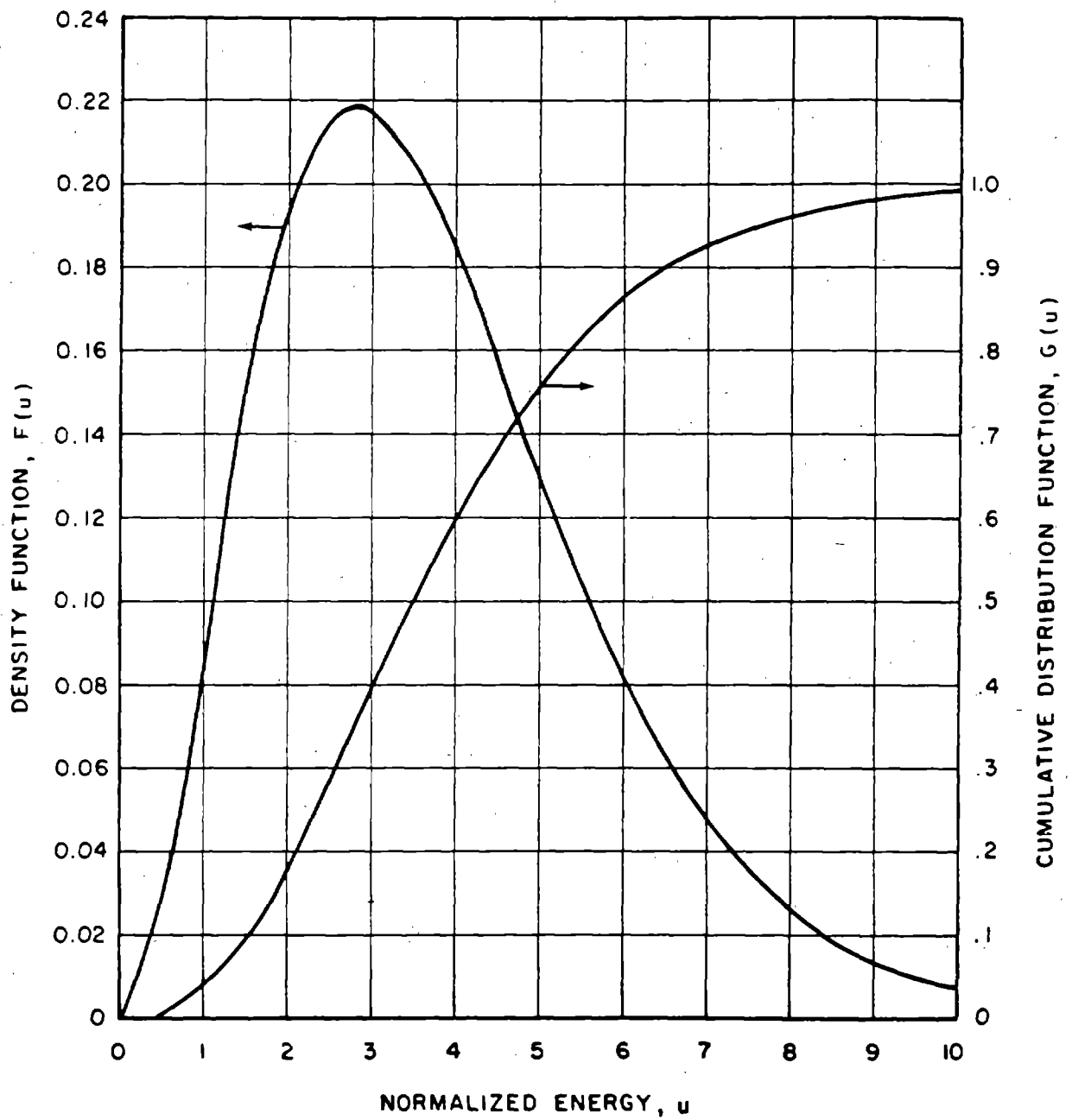


Figure 4-3. Spectral Distribution of a Black Body Source

4-3 Interactions of X-Rays with Matter

Just as X-rays are produced principally by phenomena involving electrons, the principal interactions of X-rays with matter also depend on atomic electrons.

In the photoelectric effect, an X-ray is totally absorbed; its energy is partly used in overcoming the binding energy of an atomic electron, and the remainder is imparted as kinetic energy to the electron and (to a much lesser extent) to the recoiling ion. No scattered X-ray is observed; however, the deexcitation of the ionized atom can result in secondary X-ray, ultraviolet, or optical radiation. This phenomenon is known as fluorescence. Photoelectric absorption is most probable when the X-ray energy just exceeds the binding energy of a particular electron. Thus, as the wavelength of the incident X-ray increases (the energy decreases), the probability of absorption gradually rises until the binding energy of the K-shell electron is reached. It then abruptly drops (the "K-absorption edge"), and then begins rising again until the next absorption edge is reached, and so on.

Another effect is Compton (inelastic) scattering. When an X-ray collides with an electron, it is possible that, not only a resultant energetic electron, but also a scattered X-ray photon of lower frequency (longer wavelength) will be observed. This usually happens when the target electron is free or very loosely bound. If it is assumed that the electron is free, the interaction can be analyzed as collision between two particles. Conservation of momentum and energy then yield the relation

$$\lambda' - \lambda = \frac{h}{m_0 c} (1 - \cos \theta)$$

where λ is the wavelength of the incident photon, λ' that of the scattered photon, θ the angle of scattering, and m_0 the mass of the electron (9.1×10^{-28} g).

A third effect is elastic scattering. If an electron is excited by an electromagnetic wave, it will gain energy and oscillate. As a moving charge, it will then reradiate the energy as electromagnetic radiation of the same frequency, which appear as scattered photons. The scattered photons may be coherent (in phase) or incoherent (random phases).

The probability that any of the above scattering or photoelectric processes will take place is given in terms of a cross-section σ (so called because it has units of area), which is the probability of a given interaction taking place under the condition that one interaction per unit area is possible.

If the medium with which the X-rays interact is characterized by an electron density ρ_e , then for every centimeter an X-ray traverses, there are ρ_e electrons within a cross-sectional area of one cm^2 with which it can interact. The probability of interaction per centimeter is therefore $\mu = \rho_e \sigma$. Since this is also the probability that an X-ray disappears from the incident beam, the beam intensity falls by a factor $e^{-\mu x}$ after having penetrated a distance x into the material. It is often convenient to express the penetration in terms of the total amount of material "seen" by the beam, ρx , where ρ is the mass density of the material. In this case, the mass attenuation coefficient $\kappa = \mu/\rho$ is used. The mass attenuation coefficients for air are shown as a function of X-ray photon energy in Table 4-2 and in Figure 4-4.

If the X-rays radiate isotropically from a point source rather than in a narrow beam, the flux, Φ , of X-rays (photons per unit area per unit time) at any point depends not only on the exponential attenuation described above but also on the spherical attenuation, so that

$$\Phi = Ne^{-\kappa(\rho R)}/4\pi R^2$$

where R is the radial distance from the source

[REDACTED]

Table 4-2. [REDACTED] Mass Attenuation Coefficients for Air [REDACTED]

| Photon Energy (keV) | Total Scatter (cm ² /g) | Photoelectric (cm ² /g) | Total Attenuation (cm ² /g) |
|---------------------|------------------------------------|------------------------------------|--|
| 2 | 9.791 x 10 ⁻¹ | 4.95 x 10 ² | 4.960 x 10 ² |
| 3.2* | 7.754 x 10 ⁻¹ | 1.34 x 10 ² | 1.348 x 10 ² |
| 3.2 | 7.754 x 10 ⁻¹ | 1.56 x 10 ² | 1.568 x 10 ² |
| 4 | 6.707 x 10 ⁻¹ | 8.27 x 10 ¹ | 8.337 x 10 ¹ |
| 6 | 5.070 x 10 ⁻¹ | 2.30 x 10 ¹ | 2.351 x 10 ¹ |
| 8 | 4.126 x 10 ⁻¹ | 9.54 x 10 ⁰ | 9.953 x 10 ⁰ |
| 10 | 3.529 x 10 ⁻¹ | 4.57 x 10 ⁰ | 4.923 x 10 ⁰ |
| 20 | 2.409 x 10 ⁻¹ | 4.96 x 10 ⁻¹ | 7.369 x 10 ⁻¹ |
| 40 | 1.885 x 10 ⁻¹ | 5.07 x 10 ⁻² | 2.393 x 10 ⁻¹ |
| 60 | 1.690 x 10 ⁻¹ | 1.33 x 10 ⁻² | 1.823 x 10 ⁻¹ |
| 80 | 1.569 x 10 ⁻¹ | 5.29 x 10 ⁻³ | 1.622 x 10 ⁻¹ |
| 100 | 1.480 x 10 ⁻¹ | 2.61 x 10 ⁻³ | 1.506 x 10 ⁻¹ |
| 200 | 1.210 x 10 ⁻¹ | 1.68 x 10 ⁻⁴ | 1.212 x 10 ⁻¹ |
| 400 | 9.468 x 10 ⁻² | 9.80 x 10 ⁻⁶ | 9.469 x 10 ⁻² |
| 600 | 8.014 x 10 ⁻² | 3.92 x 10 ⁻⁶ | 8.014 x 10 ⁻² |

*Argon K-Absorption Edge.

[REDACTED]

and N is the total number of photons emitted by the source per unit time. This, however, is only the component that reaches the point directly from the source. Scattered photons (coherent, incoherent, and Compton) originating at other points also reach the point. The result is that the flux of that point is larger by a buildup factor B . The magnitude of B depends on the distance from the source, the energy spectrum of the X-rays, and properties of the scattering material in complex ways. It is ordinarily calculated by computer codes. The integral of the flux over time, or the total number of X-ray photons per unit area reaching a point, is known as the

fluence. *Flux and fluence are also commonly described in terms of the energy carried by the photons instead of their number.*

SECTION I

[REDACTED] NUCLEAR WEAPONS AS X-RAY SOURCES [REDACTED]

4-4 X-Ray Production in Nuclear Weapons [REDACTED]

[REDACTED] The multitude of processes that occur very early in the detonation of a nuclear weapon are described in Chapter 1. The result,

[REDACTED]

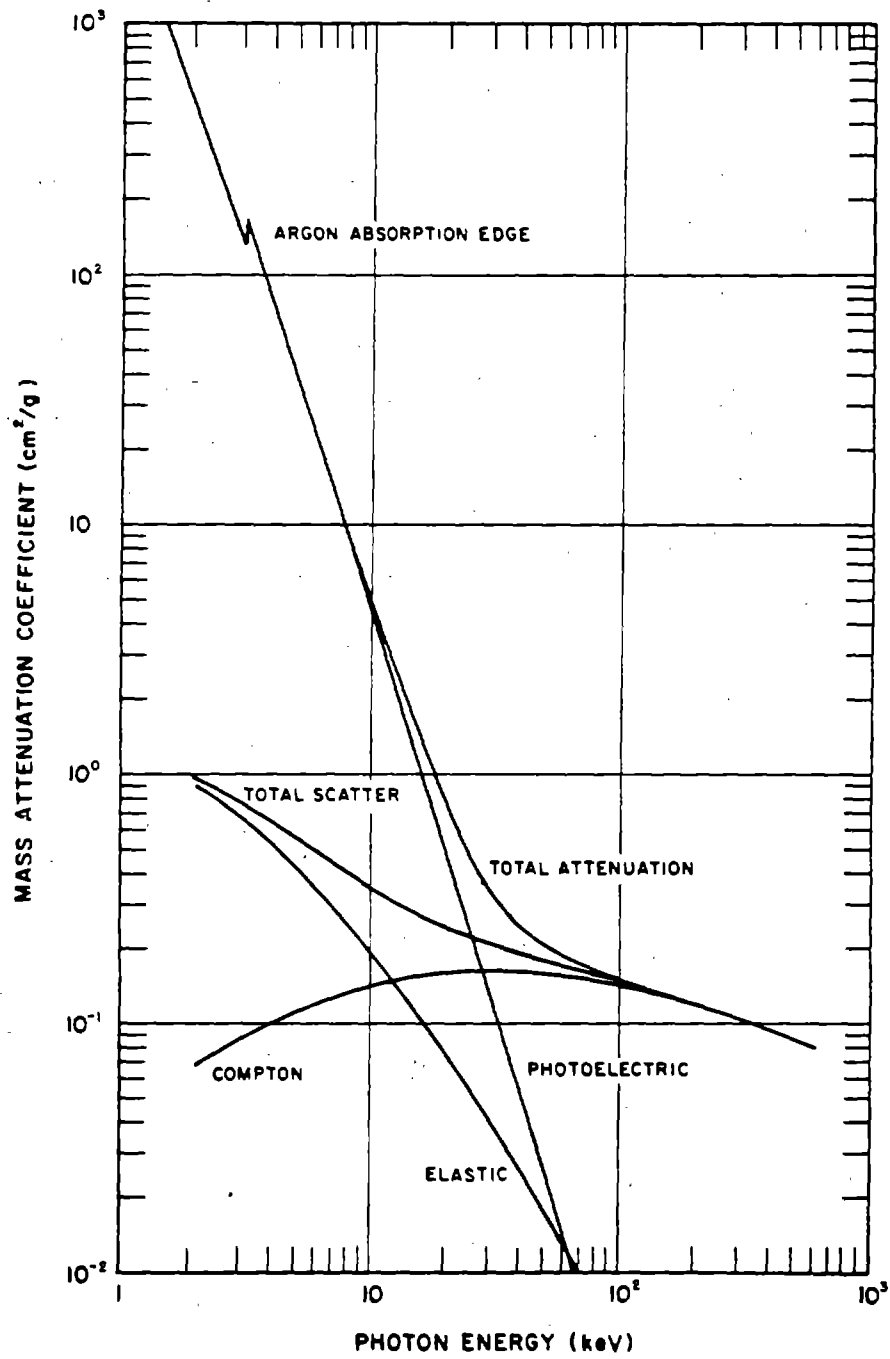


Figure 4-4. [REDACTED] Mass Attenuation Coefficients for Air [REDACTED]

[REDACTED]

[REDACTED]

[REDACTED]

as far as X-ray production is concerned, is that a very hot (tens of millions of degrees Kelvin) plasma is formed, consisting of electrons and the stripped nuclei of the fission and fusion products, of the elements in the casing materials, and of any other elements in the immediate vicinity of the detonation, such as nitrogen and oxygen in the air. Although the spectrum of emissions from this plasma is not that of a black body, particularly because the temperature is by no means uniform, it often approximates a black body spectrum, or a combination of two or more such spectra. The disposition of X-rays is further complicated by interactions with the atmosphere.

Approximately 70 to 80 percent of the total prompt yield of many nuclear weapons is radiated in the form of X-rays.

In recent years, considerable attention has been devoted to designing "hot" nuclear weapons with effective radiation temperatures greater than

4-5 X-Ray Energy Emitted

A temperature gradient, decreasing outward, exists between the enormously hot interior nuclear materials and the somewhat cooler exterior bomb casing materials of the nuclear weapon. The X-rays, of course, are continuously being absorbed and reradiated, but with a temperature gradient, the conditions for an ideal black body with isotropic radiation at every point do not exist, and there is a net flow of energy outward from the point of detonation. The outward flux at the surface is, in fact, about twice what would be implied by black body radiation at the temperature of the surface because of X-rays from the interior escaping without interaction at the surface. If the actual surface temperature is T_s , then the surface energy flux is given by

$$\Phi_s = \sigma T_e^4$$

where

$$T_e = 2^{1/4} T_s = 1.19 T_s.$$

The effective temperature, T_e , will be used in the succeeding discussions.

4-6 Rate of X-Ray Emission

[REDACTED]

[REDACTED]

DNA
(S)(3)

[REDACTED]

Similarly, the effective X-ray temperature and equivalent black body fluence may be obtained from experimental measurements

[REDACTED]

DNA
(S)(3)

Actually, radiation cannot continue at the peak emission rate because the loss of energy cools the plasma and it radiates correspondingly less rapidly as time goes on. The time necessary to radiate a given fraction (about 90 percent) of the weapon energy increases with the size of the emitting sphere (r), and of course is larger than the time calculated from the peak emission rate; however, it is still generally measured in shakes or tenths of a shake for most weapons.

4-7 Spectral Distribution of X-Rays

An approximation of the X-ray spectra from nuclear weapons can be obtained from the normalized Planck distribution by applying the appropriate multiplicative factors to the independent (u) and dependent (F and G) variables for the black body temperature indicated (see paragraph 4-2).

This example is given in more detail in Problem 4-3. The equivalent black body spectrum can now be constructed and compared with the rest of the measured spectrum. Some examples of such comparisons will be shown in subsequent paragraphs.

For the purpose of calculating X-ray effects, the spectrum is most useful if tabulated by intervals in u enclosing approximately equal energy increments of the cumulative distribution function. In such computations, each increment is treated as being composed of monoenergetic photons of the central energy. Table 4-3 shows the boundaries of the energy intervals for approximately five percent increments of the normalized cumulative distribution function and the corresponding boundaries of photon energies for several source temperatures. Five percent increments may be too coarse for estimating effects both at the very low and very high ends of the spectrum. For these regions, the one percent increments shown in Table 4-4 may be useful.

4-8 Real Nuclear Weapons as X-Ray Sources

Since X-rays are attenuated rapidly by air, very little can be ascertained about the initial properties of nuclear weapons as X-ray sources from atmospheric weapons tests. However, X-ray effects may constitute the principal kill mechanism for high altitude interception of ballistic missiles

DNA
(S)(3)

[REDACTED]

[REDACTED]

Page 4-13 is deleted.

Table 4-3. Five Percent Energy Intervals for a Planck Spectrum

| Cumulative Distribution Function | Photon Energy in keV for Various Black Body Temperatures | | | |
|--|---|-------|-------|--------|
| | 1 keV | 2 keV | 8 keV | 10 keV |
| 0 | 0 | 0 | 0 | 0 |
| 0.0506 | 1.16 | 2.32 | 9.28 | 11.60 |
| 0.1008 | 1.54 | 3.08 | 12.32 | 15.40 |
| 0.1511 | 1.84 | 3.68 | 14.72 | 18.40 |
| 0.2007 | 2.10 | 4.20 | 16.80 | 21.00 |
| 0.2500 | 2.34 | 4.68 | 18.72 | 23.40 |
| 0.3013 | 2.58 | 5.16 | 20.64 | 25.80 |
| 0.3493 | 2.80 | 5.60 | 22.40 | 28.00 |
| 0.4017 | 3.04 | 6.08 | 24.32 | 30.40 |
| 0.4491 | 3.26 | 6.52 | 26.08 | 32.60 |
| 0.4994 | 3.50 | 7.00 | 28.00 | 35.00 |
| 0.5515 | 3.76 | 7.52 | 30.08 | 37.60 |
| 0.6007 | 4.02 | 8.04 | 32.16 | 40.20 |
| 0.6499 | 4.30 | 8.60 | 34.40 | 43.00 |
| 0.7010 | 4.62 | 9.24 | 36.96 | 46.20 |
| 0.7519 | 4.98 | 9.96 | 39.84 | 49.80 |
| 0.8004 | 5.34 | 10.68 | 42.62 | 53.80 |
| 0.8499 | 5.88 | 11.76 | 47.04 | 58.80 |
| 0.9003 | 6.56 | 13.12 | 52.48 | 65.60 |
| 0.9500 | 7.64 | 15.28 | 61.12 | 76.40 |

DNA
(1)(3)

DNA
(1)(3)

Figures 4-6 through 4-11 show some X-ray spectra from real nuclear weapons, both observed and predicted. Figure 4-6 shows the observed spectrum of a warm X-ray weapon.

DNA
(1)(3)

Table 4-4. One-Percent Energy Intervals for a Planck Spectrum

| Cumulative Distribution Function | Photon Energy in keV for Various Black Body Temperatures | | | |
|--|---|-------|-------|--------|
| | 1 keV | 2 keV | 8 keV | 10 keV |
| 0.0105 | 0.64 | 1.28 | 5.12 | 6.40 |
| 0.0205 | 0.82 | 1.64 | 6.56 | 8.20 |
| 0.0295 | 0.94 | 1.88 | 7.52 | 9.40 |
| 0.0402 | 1.06 | 2.12 | 8.48 | 10.60 |
| 0.0506 | 1.16 | 2.32 | 9.28 | 11.60 |
| 0.0597 | 1.24 | 2.48 | 9.92 | 12.40 |
| 0.0697 | 1.32 | 2.64 | 10.56 | 13.20 |
| 0.0804 | 1.40 | 2.80 | 11.20 | 14.00 |
| 0.0903 | 1.47 | 2.94 | 11.76 | 14.70 |
| 0.1008 | 1.54 | 3.08 | 12.32 | 15.40 |
| 0.9003 | 6.56 | 13.12 | 52.48 | 65.60 |
| 0.9098 | 6.72 | 13.44 | 53.76 | 67.20 |
| 0.9200 | 6.91 | 13.82 | 55.28 | 69.10 |
| 0.9300 | 7.12 | 14.24 | 56.96 | 71.20 |
| 0.9401 | 7.36 | 14.72 | 58.88 | 73.60 |
| 0.9502 | 7.64 | 15.28 | 61.12 | 76.40 |
| 0.9598 | 7.96 | 15.92 | 63.68 | 79.60 |
| 0.9700 | 8.39 | 16.78 | 67.12 | 83.90 |
| 0.9801 | 8.98 | 17.96 | 71.84 | 89.80 |
| 0.9900 | 9.94 | 19.88 | 79.52 | 99.40 |

DNA
(A)(3)

DNA
(A)(3)

Pages 4-16 through 4-24 are deleted. 4-15

[REDACTED]

SECTION II
X-RAY ENVIRONMENTS
PRODUCED BY NUCLEAR WEAPONS

4-9 Exoatmospheric (Vacuum)
Detonations

[REDACTED] X-ray environments from nuclear detonations are completely specified by the magnitude of the source and the distance from the source to the point of interest if the detonation occurs in a vacuum. If the detonation occurs at an altitude sufficiently high that essentially vacuum conditions prevail, it is designated an exoatmospheric detonation. Since, in any case, the vacuum will be less than perfect, the distinction between exoatmospheric and endoatmospheric detonations will depend on the degree to which effects vary from those predicted for a vacuum. This will depend on weapon design features, particularly whether the X-ray spectrum is hot or cold.

[REDACTED] For perfect vacuum conditions, the X-ray energy fluence at a range R from the point of detonation is

$$\phi = \frac{E_0}{4\pi R^2} \text{ cal/cm}^2$$

where E_0 is the X-ray yield of the weapon in calories and R is the distance in centimeters. If E_0 is not known, it may be estimated as 75 percent of the total yield of the weapon. Using the relationship that 1 kt = 10^{12} calories, the vacuum fluence is shown as a function of distance from detonations of various x-ray yields in Figure 4-12. The fluence may also be calculated from the equation

$$\phi = \frac{85.7 W'_x}{R_f^2}$$

where W'_x is the X-ray yield in kilotons and R_f is the range in kilofeet.

[REDACTED] Since no interactions can take place in an empty medium, no changes in the spectral distribution of X-rays occurs in exoatmospheric detonations. For the same reason, the time dependence of X-ray energy flux is unchanged, and the time of arrival of the pulse at range R is R/c , where c is the velocity of light. Since, for the calculation of effects, only times relative to the arrival time are important, the only variation of effects with range is due to the variation in total fluence.

4-10 Endoatmospheric Detonations

[REDACTED] The X-ray environment produced by nuclear detonations within the atmosphere are much more complicated because of the many interactions that can take place between the X-rays and the atmospheric constituents. Photoelectric absorption, elastic scattering, and inelastic (Compton) scattering all play a part in altering the total X-ray fluence that reaches a given range, the spectral distribution at that point, and the time rate of energy delivery. Density gradients and other inhomogeneities in the atmosphere cause the X-ray environment to deviate from the spherical symmetry exhibited in vacuum detonations. Because of scattering, the X-ray photons arriving at a given point do not all arrive from the direction of the detonation; in fact, some may arrive from precisely the opposite direction.

4-11 The Standard Atmosphere

[REDACTED] The estimation of X-ray environments around an endoatmospheric nuclear detonation requires a knowledge of the atmospheric properties along any path that an X-ray photon might traverse from the weapon to the point of interest. Although atmospheric properties can change somewhat from day to day and place to place, most calculations are based on a standard atmosphere such as the one described by the National Bureau of Standards in 1962. The im-

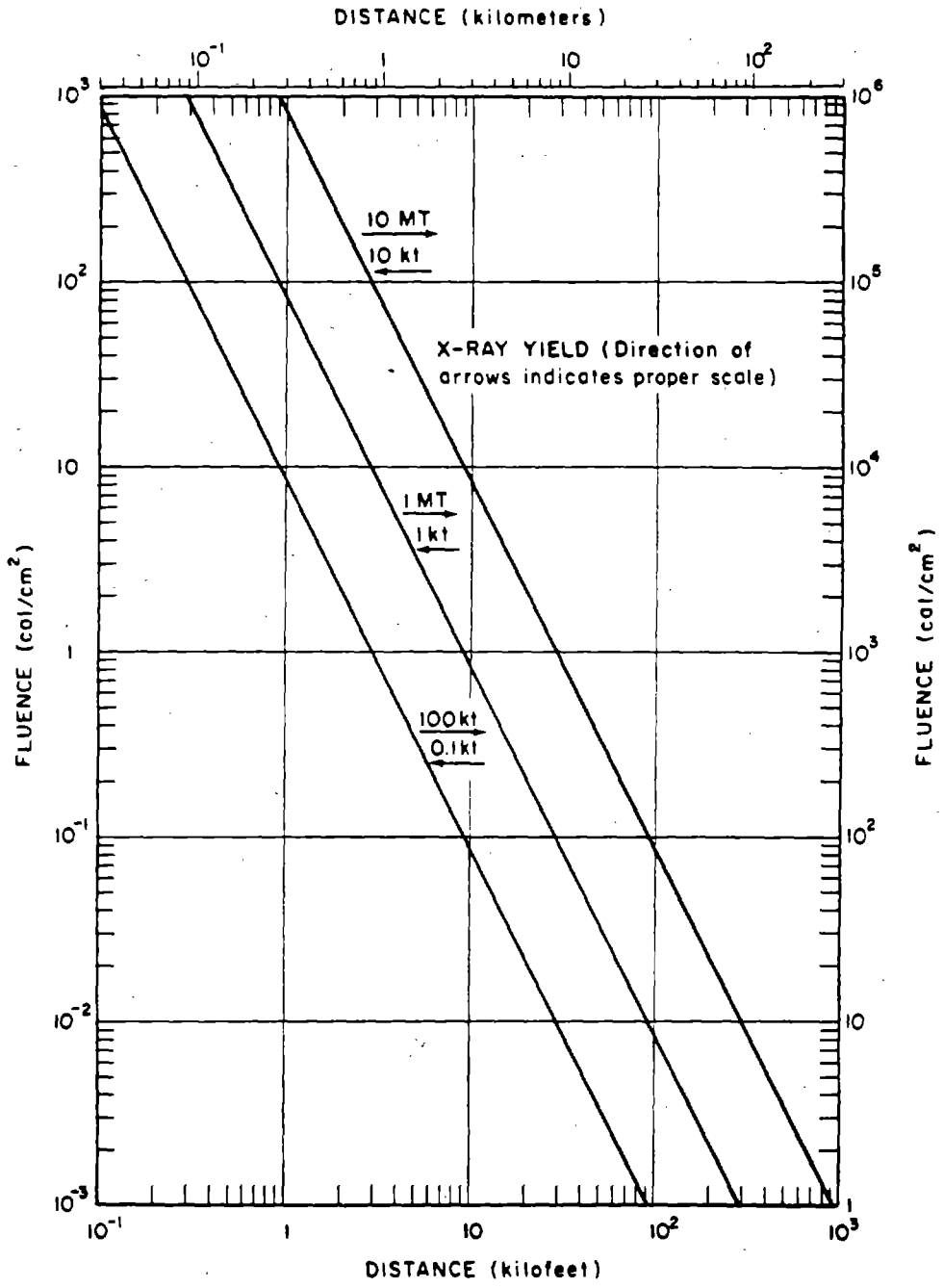
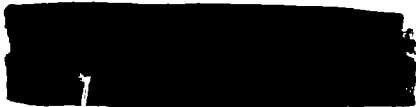
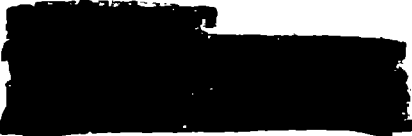


Figure 4-12. X-Ray Fluence in a Vacuum



portant atmospheric constituents are

| | Fraction by Weight |
|----------|-----------------------|
| Nitrogen | 0.7553 |
| Oxygen | 0.2318 |
| Argon | 0.0129 |

Argon is included because its photoelectric absorption cross section for X-rays is large and serious errors can be made if it is neglected. The other minor components of the atmosphere, however, can be neglected without serious loss of accuracy.

The other principal feature of the standard atmosphere is its variation in density with altitude. The density, ρ , falls approximately exponentially with increasing altitude, as is shown in Table 4-5 and Figure 4-13. Also shown is the quantity of air above a given altitude, h , which is given by the mass integral

$$q(h) = \int_h^{\infty} \rho(h') dh'$$

Table 4-5 also shows the density normalized to the sea level density, ρ_0 .

If two points are at altitudes h_1 and h_2 and are separated by a horizontal distance, d , then the slant range R is given by

$$R = \sqrt{d^2 + (h_2 - h_1)^2}$$

and the mass integral between them is given by

$$q(R) = \int_0^R \rho(h') ds' = R \frac{q(h_2) - q(h_1)}{h_2 - h_1}$$

This expression reduces to

$$q(R) = q(h_2) - q(h_1)$$

when $d = 0$ and (in the limit) to

$$q(R) = \rho(h)R$$

when $h_1 = h_2$ (the coaltitude case).

These values for the mass integral between the source of X-rays and the point of observation are to be used for the quantity ρR in the flux or fluence attenuation equations as described in paragraph 4-3. When the mass integral is used instead of the absolute range, the X-ray environment is substantially independent of other parameters; this property is known as mass integral scaling.

4-12 Direct X-Ray Fluence in the Atmosphere

If the attenuation equations are combined with the results for vacuum fluence, the direct fluence from a weapon with W_x kilotons of X-ray yield is

$$\varphi_{\text{dir}} = \frac{85.7 W_x}{R_f^2} e^{-\kappa q(R)}$$

at a range R , where q is the mass integral calculated along R and κ is the mass attenuation coefficient. Notice that q will not be the same for different directions of R unless the atmosphere is essentially uniform, so that contours of constant fluence usually are not spherically symmetric about the burst point, although they usually are cylindrically symmetric about a vertical axis.

Moreover, the value of the mass attenuation coefficient κ varies with X-ray photon energy according to the curve shown in Figure 4-4, so that the direct fluence must be calculated by weighting monoenergetic calculations by the spectral distribution. For a given penetration of the atmosphere, $q(R)$, this weighting process can be replaced by using an effective κ , but the value of this effective κ will change with $q(R)$. Similar-

Table 4-5. The Standard Atmosphere

| Altitude (kft) | Air Density (g/cm ³) | Mass Integral Above Altitude (g/cm ²) | Density Normalized to Sea Level |
|----------------|----------------------------------|---|---------------------------------|
| 0 | 1.2250 x 10 ⁻³ | 1.0331 x 10 ³ | 1.0000 x 10 ⁰ |
| 5 | 1.0556 x 10 ⁻³ | 8.5967 x 10 ² | 8.6170 x 10 ⁻¹ |
| 10 | 9.0477 x 10 ⁻⁴ | 7.1059 x 10 ² | 7.3859 x 10 ⁻¹ |
| 20 | 6.5312 x 10 ⁻⁴ | 4.7525 x 10 ² | 5.3316 x 10 ⁻¹ |
| 30 | 4.5904 x 10 ⁻⁴ | 3.0749 x 10 ² | 3.7473 x 10 ⁻¹ |
| 40 | 3.0267 x 10 ⁻⁴ | 1.9305 x 10 ² | 2.4708 x 10 ⁻¹ |
| 50 | 1.8756 x 10 ⁻⁴ | 1.1973 x 10 ² | 1.5311 x 10 ⁻¹ |
| 60 | 1.1628 x 10 ⁻⁴ | 7.4292 x 10 ¹ | 9.4919 x 10 ⁻² |
| 70 | 7.1742 x 10 ⁻⁵ | 4.6182 x 10 ¹ | 5.8565 x 10 ⁻² |
| 80 | 4.4174 x 10 ⁻⁵ | 2.8855 x 10 ¹ | 3.6060 x 10 ⁻² |
| 90 | 2.7391 x 10 ⁻⁵ | 1.8151 x 10 ¹ | 2.2360 x 10 ⁻² |
| 100 | 1.7101 x 10 ⁻⁵ | 1.1493 x 10 ¹ | 1.3960 x 10 ⁻² |
| 110 | 1.0647 x 10 ⁻⁵ | 7.3417 x 10 ⁰ | 8.6918 x 10 ⁻³ |
| 120 | 6.6487 x 10 ⁻⁶ | 4.7534 x 10 ⁰ | 5.4275 x 10 ⁻³ |
| 130 | 4.2214 x 10 ⁻⁶ | 3.1247 x 10 ⁰ | 3.4460 x 10 ⁻³ |
| 140 | 2.7222 x 10 ⁻⁶ | 2.0831 x 10 ⁰ | 2.2222 x 10 ⁻³ |
| 150 | 1.7810 x 10 ⁻⁶ | 1.4070 x 10 ⁰ | 1.4539 x 10 ⁻³ |
| 160 | 1.1968 x 10 ⁻⁶ | 9.5903 x 10 ⁻¹ | 9.7697 x 10 ⁻⁴ |
| 180 | 5.6991 x 10 ⁻⁷ | 4.4396 x 10 ⁻¹ | 4.6523 x 10 ⁻⁴ |
| 200 | 2.7163 x 10 ⁻⁷ | 1.9859 x 10 ⁻¹ | 2.2174 x 10 ⁻⁴ |
| 250 | 3.6248 x 10 ⁻⁸ | 2.0476 x 10 ⁻² | 2.9590 x 10 ⁻⁵ |
| 300 | 2.3839 x 10 ⁻⁹ | 1.5137 x 10 ⁻³ | 1.9460 x 10 ⁻⁶ |
| 400 | 1.8645 x 10 ⁻¹¹ | 2.7532 x 10 ⁻⁵ | 1.5220 x 10 ⁻⁸ |
| 500 | 1.6329 x 10 ⁻¹² | 6.2391 x 10 ⁻⁶ | 1.3330 x 10 ⁻⁹ |
| 1,000 | 3.2769 x 10 ⁻¹⁴ | 0 | 2.6750 x 10 ⁻¹¹ |

ly, the spectrum changes as matter is traversed because of the varying proportions of photons absorbed or scattered out of the flux at varying photon energies.

In practice, the most accurate method for calculating fluences uses Monte Carlo com-

puter codes with accurate photon cross sections for each energy group and each scattering or absorbing process. This technique is also essential for following those X-ray photons scattered out of the direct fluence, as will be discussed subsequently.

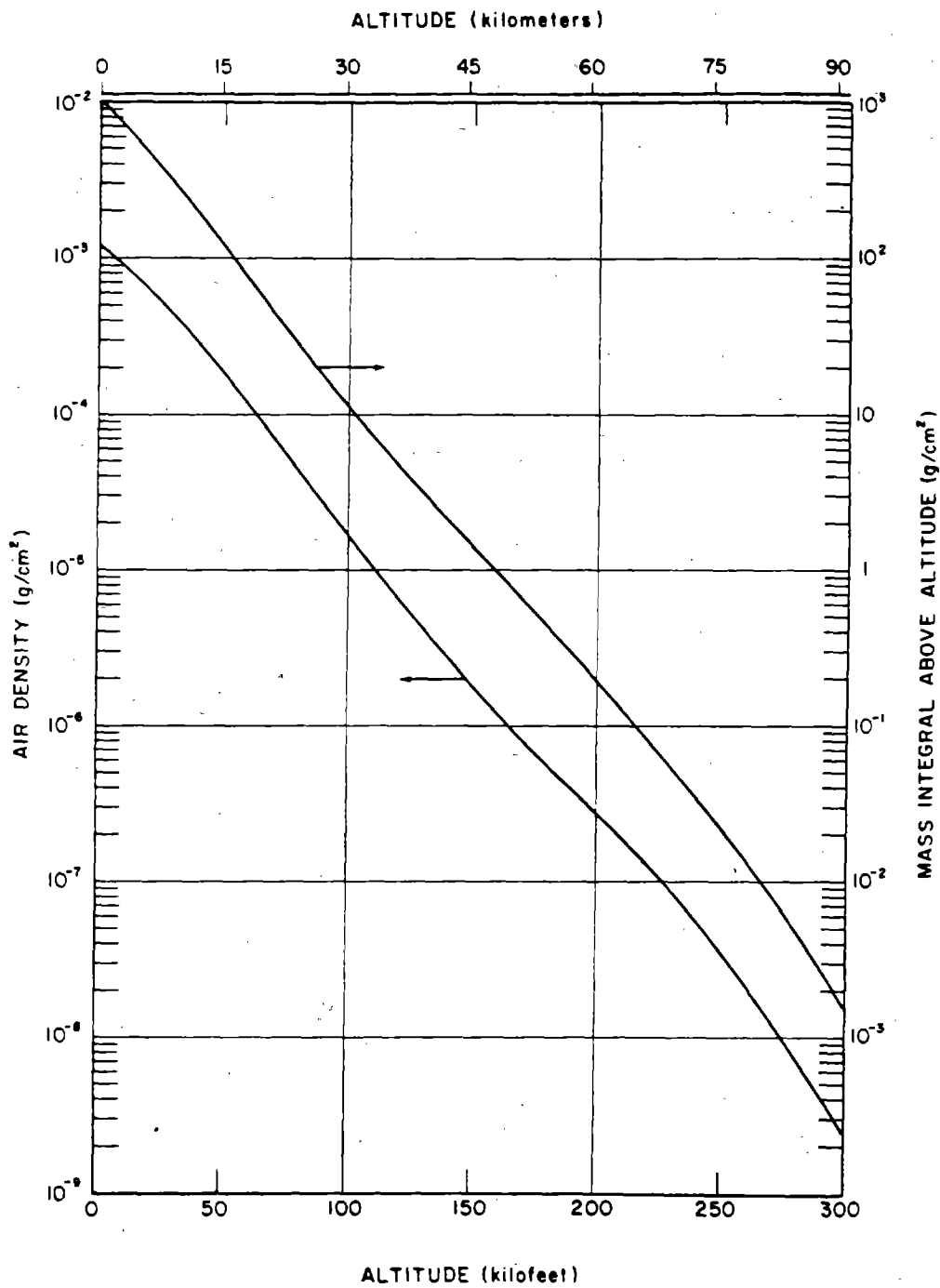
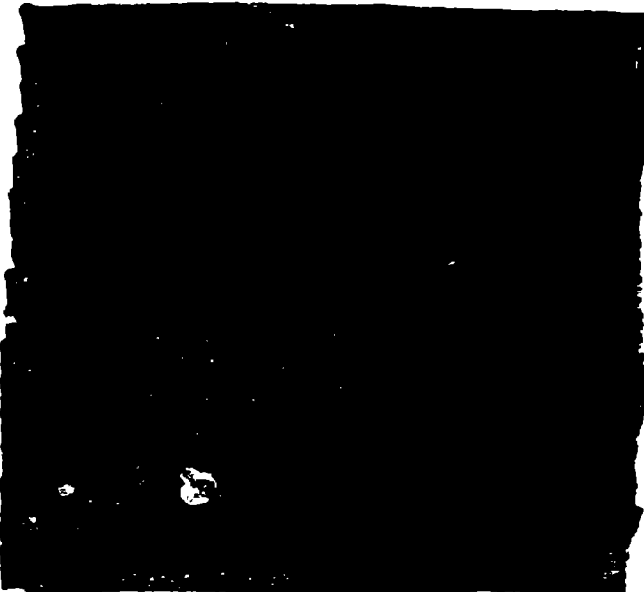


Figure 4-13. The Standard Atmosphere

[REDACTED]

DATA
(L)(3)



addition to the spherical divergence, which is not included since the fraction of vacuum fluence is the quantity shown). The build-up factor, which includes photons of degraded energy, rises so rapidly that the total fluence for short ranges actually exceeds that expected for the vacuum case, in which only spherical divergence would be operating. Figure 4-15 and 4-16 show results for black body source spectra, also normalized to the vacuum fluence. Notice that the direct fluences are no longer exponential, although in the latter case a mass attenuation coefficient corresponding to about five times the black body temperature gives reasonable results. The normalized fluences for the latter two cases are also tabulated in Table 4-6.

4-13 Scattered X-Ray Fluence

The X-rays arriving at a given point come not only directly from the source but also indirectly (and usually from other directions) after one or more scattering events. The probabilities of scattered photons contributing to the flux depends on the total cross sections for scattering and the differential cross sections for scattering at specific angles. The flux of scattered photons is usually computed by a Monte Carlo simulation of the paths taken by a representative sample of photons, taking into account also the possibility of degradation of energy in Compton scattering. The resultant flux adds to that penetrating directly from the source, and the ratio of the total fluence to the direct fluence is known as the build-up factor. The build-up factor increases from unity very near the source to more than one hundred for longer ranges.

No simple analytic expression gives the build-up factor, but Figures 4-14 through 4-16 give direct and total fluences and the build-up factor for three representative X-ray sources. In the monoenergetic source case (Figure 4-14), the direct fluence is attenuated exponentially (in

[REDACTED]

The cold X-rays are attenuated much more quickly in air, because the mass attenuation coefficient is so much larger for lower energies.

[REDACTED]

DATA
(L)(3)

DATA
(L)(3)

4-14 Low Altitude Endoatmospheric Detonations

Low altitude (deep) endoatmospheric detonations are the next simplest case - after vacuum detonations - because the air density is sufficiently high that most of the attenuation occurs close to the burst point. Therefore, there are no large variations in density to affect critically the computation of fluences. In particular, the density of air through which the scattered X-rays reach a given point does not differ greatly from that through which the direct X-rays penetrate. Although whether or not altitudes are low (detonations are deep) depends on the energy

[REDACTED]

[REDACTED]

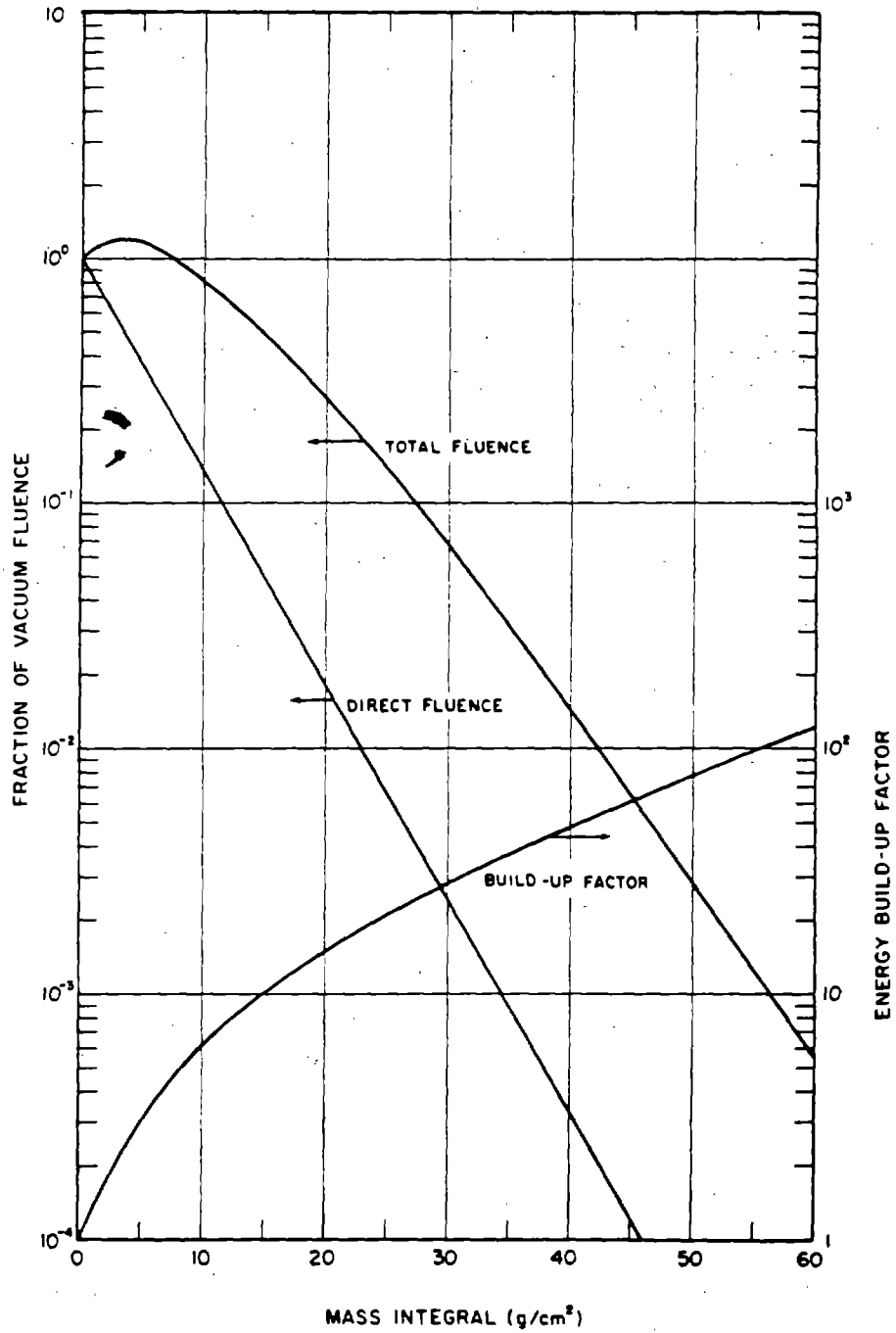


Figure 4-14. Energy Fluence and Build-up Factor for a 50 keV Monoenergetic Source in Homogeneous Air

Pages 4-32 + 4-33 are deleted. 4-31

[REDACTED]

Table 4-6. [REDACTED] X-Ray Fluences for Black Body Sources [REDACTED]

DNA
(A)(3)

[REDACTED TABLE]

spectrum of the weapon, if deep endoatmospheric conditions do prevail, the X-ray environment can be approximated by mass integral scaling. The total quantity of air (the mass integral) between the source and the point of interest is computed as described in paragraph 4-11, and then the appropriate direct and scattered fluences for the given energy spectrum are calculated as described in paragraphs 4-12 and 4-13. Examples of such calculations are provided in Problems 4-5 and 4-6. Less detailed examples are discussed in the following paragraphs.

[REDACTED]

DNA
(E)(3)

The fluences for the same mass-integrally scaled distances in directions other than horizontal are approximately the same. For instance, the actual distance to the 10 cal/cm² contour will be somewhat larger vertically upward than horizontally because the air is somewhat less dense; conversely, the distance vertically downward will be somewhat smaller. The resulting fluence contours are egg-shaped.

Furthermore, the computed fluences will be even more accurate at the same mass-integrally scaled distances as the burst point falls lower in the atmosphere. The X-ray fluence contours will tend to become more spherical and contract because of the increasing air density. On the other hand, the reliability of the computations decreases as the burst altitude increases above 100 kilofeet.

DNA
(E)(3)

[REDACTED]

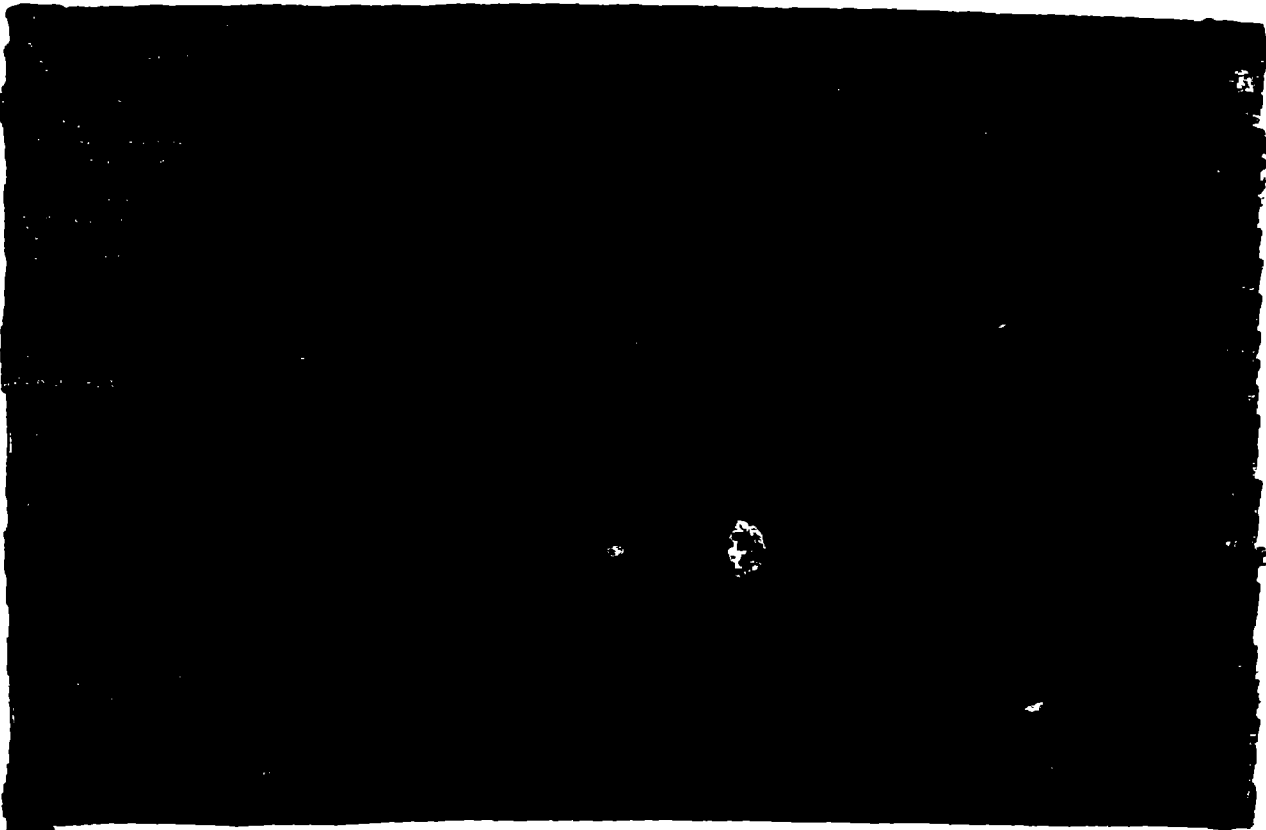
[REDACTED]

DNA
(E)(3)

[REDACTED]

[REDACTED]

[REDACTED]

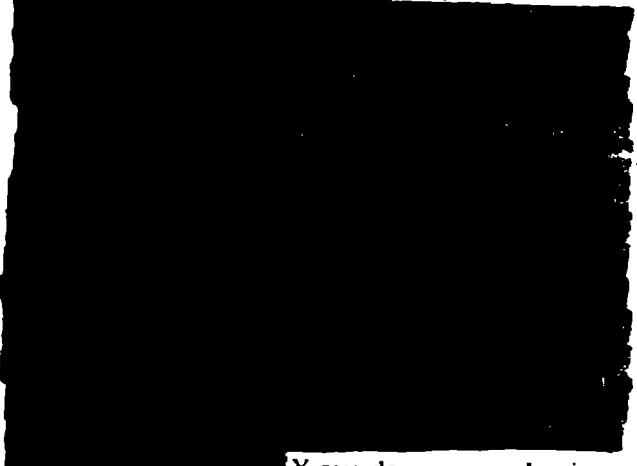
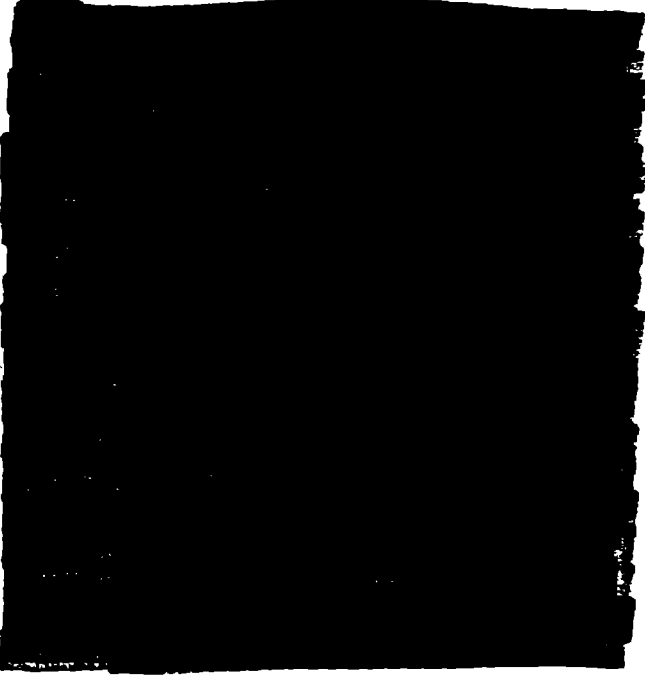


DNA
(L)(3)

○

[REDACTED] X-ray effects on materials may depend on several variables in the X-ray environment

DNA
(L)(3)



DNA
(L)(3)

[REDACTED] X-ray damage mechanisms are discussed in Section V of Chapter 9.

[REDACTED] The spectrum of the direct fluence tends to become harder – that is, its proportion of

[REDACTED]

[REDACTED]

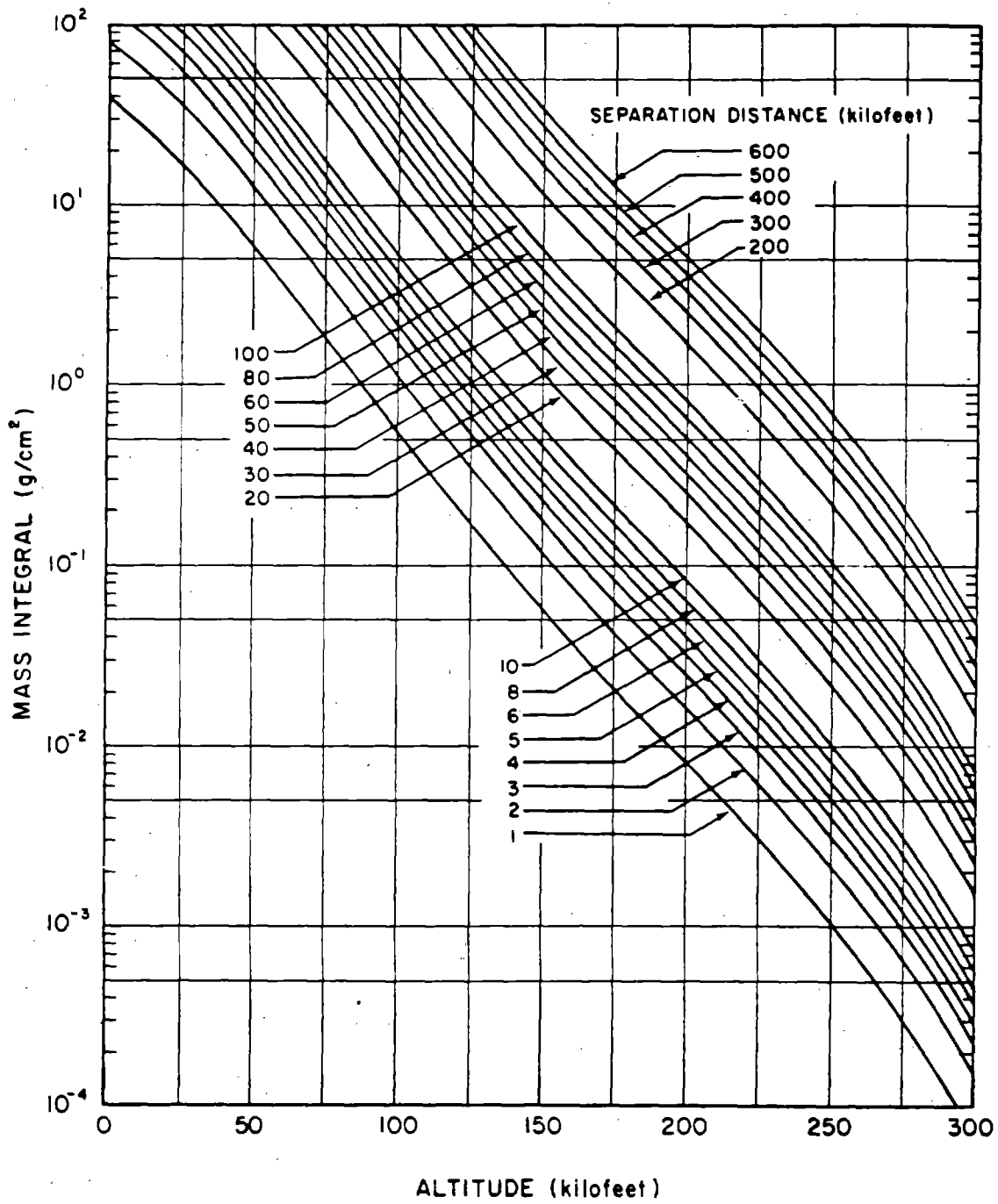


Figure 4-17 [redacted] Mass Integral for Specified Coaltitude Separation Distances as a Function of Altitude [redacted]

[REDACTED]

DNA
(A)(3)

Deleted

Figure 4-18. [REDACTED] Transmission of Direct X-Ray Fluence Through
Air for Various Black Body Sources [REDACTED]

[REDACTED]

[REDACTED]

[REDACTED]

DNA
(b)(3)

Deleted

Figure 4-19. [REDACTED] X-Ray Fluence Through Air for
[REDACTED] Various Black Body Sources

[REDACTED]

[REDACTED]

[REDACTED]

high energy X-rays increases – as the mass of air penetrated increases. This phenomenon occurs because the higher cross sections, particularly for photoelectric absorption, occur at lower energies and preferentially remove low energy X-rays from the direct fluence. However, every Compton scattering process degrades the energy of the scattered photon, and the scattered component of the fluence tends to become increasingly soft as the penetration increases. These two effects partially compensate for one another, and the typical black body spectrum is little affected by passage through air.

[REDACTED] The rate of X-ray production from nuclear weapons as sources has already been discussed in paragraph 4-6.

DNA
(K-)(3)

[REDACTED]

Because the scattered component is softer than the direct component and arrives later, the spectrum of X-rays incident also varies with time in a complex fashion, and the dependence varies with the quantity of air traversed. Similarly, the direct fluence is all moving radially out-

ward from the source, whereas the scattered photons can be incident from all directions, even from directly opposite the source. Thus the fraction of the energy flux moving outward (angles less than 90° from the radial vector) varies with time and location. In general, the fraction decreases from unity as time increases. However, when all times are considered, about 80 percent of the total fluence is outward for most ranges, and the fact that a portion of the fluence is backscattered can be neglected for most applications.

4-15 High Altitude Endoatmospheric Detonations [REDACTED]

[REDACTED] When nuclear detonations are so high that mass integral scaling is not correct, but yet sufficiently endoatmospheric that vacuum conditions are not satisfied, special and detailed calculations must be made for each case of interest. Although mass integral scaling is applicable for the direct fluence, the scattered component traverses paths of varying composition, and detailed Monte Carlo computer codes are necessary to describe the interactions.

[REDACTED] *DNA*
(K-)(3)

The spectrum of Figure 4-10 was used. In computing horizontal ranges, the curvature of the earth was considered. The resulting total fluence contours are shown in Figure 4-21. Contours for the mass integral are also shown. Vacuum fluences and attenuation factors can be computed and direct fluences predicted from these contours.

Pages 4-40 through 4-44 are deleted.

[REDACTED]

Problem 4-5. Calculation of Direct Fluence in the Atmosphere

[REDACTED] Because every interaction of a photon with the material it traverses takes it out of the beam, the attenuation of *direct* fluence is exponential with the mass integral traversed, for a given energy of X-ray photon. Changes in spectral shape can be computed by calculating the contributions of the various energy components as the atmosphere is penetrated. As discussed in paragraph 4-12, the weighting of monoenergetic components becomes laborious for complex spectra, and these calculations usually are performed with computer codes. For this reason, a very simple example has been chosen to illustrate the procedures.

Example

[REDACTED]

[REDACTED]

DNA
(4-)(3)

Pages 4-46 and 4-47 are deleted. 4-45

[REDACTED]

[REDACTED]

[REDACTED]

[REDACTED] **BIBLIOGRAPHY** [REDACTED]

Christian, R. H., and P. G. Fischer, *Phenomenology Estimates and a Proposed Experimental Program for Sentinel Environment Tests* [REDACTED] DASA 2116, 68TMP-30, General Electric Company, TEMPO, Santa Barbara, California, 29 February 1968 [REDACTED]

[REDACTED]

Evans, B. S. and F. H. Shelton, *A Table of the Planck Radiation Function and Its Integral*, KN-770-70-36, Kaman Nuclear, Colorado Springs, Colorado, 2 February 1970 [REDACTED]

[REDACTED]

Gilmore, F. R., *A Table of the Planck Radiation Function and Its Integral*, RM-1743, RAND Corporation, Santa Monica, California, 2 July 1956 [REDACTED]

Latter, A. L., *Another Vulnerability* [REDACTED] RM-3981-PR, RAND Corporation, January 1964 [REDACTED]

Latter, A. L., *A High Temperature Nuclear Weapon* [REDACTED] RM-3978-AEC, RAND Corporation, Santa Monica, California, 23 December 1963 [REDACTED]

LRL Warheads for Advanced Spartan [REDACTED] LRL-CMA 68-154, Lawrence Radiation Laboratory, Livermore, California, 31 October 1968 [REDACTED]

Shelton, F. H., *Some Notes on the Spectral Distribution of Blackbody Sources* [REDACTED] KN-655-65-12, Kaman Nuclear, Colorado Springs, Colorado, 31 March 1965 [REDACTED]

[REDACTED]

Shelton, F. H., and J. R. Keith, *X-Ray Air Transport* [REDACTED] DASA 1981, KN-717-67-1, Kaman Nuclear, Colorado Springs, Colorado, 1 July 1967 [REDACTED]

[REDACTED]

Shelton, F. H., and J. R. Keith, *Time Dependent X-Ray Air Transport* [REDACTED] DASA 2138, KN-717-68-4, Kaman Nuclear, Colorado Springs, Colorado, 31 May 1968 [REDACTED]

[REDACTED]

Shelton, F. H., and J. R. Keith, *Initial Radiation Environments Produced by SPARTAN Events and Some of Their Aerospace Systems Effects* [REDACTED] DASA 2371, KN-774-69-4, Kaman Nuclear, Colorado Springs, Colorado, 24 July 1969 [REDACTED]

[REDACTED]

Shelton, F. H., *Nuclear Weapons as X-Ray Sources, the Environments They Produce, and Some Effects on Aerospace Systems* [REDACTED] Volume I - X-Ray Sources and the Environments They Produce [REDACTED] DASA 2397-1, KN-770-69-30, Kaman Nuclear, Colorado Springs, Colorado, September 1969 [REDACTED]

[REDACTED]

U.S. Standard Atmosphere, 1962, U.S. Committee on Extension to the Standard Atmosphere, available through the U.S. Government Printing Office, December 1962 [REDACTED]

[REDACTED]

U.S. Standard Atmosphere Supplements, 1966, U.S. Committee on Extension to the Standard Atmosphere, available through the U.S. Government Printing Office, 1966 [REDACTED]

[REDACTED]



This page intentionally left blank

